

THERMOELECTRIC PROPERTIES OF Cu-DISPERSED $\text{Bi}_2\text{Te}_{2.7}\text{Se}_{0.3}$ NANOCOMPOSITES

Il-Ho Kim^{1*}, Soon-Mok Choi², Won-Seon Seo², Dong-Ik Cheong³, Hyung Kang³

¹ Department of Materials Science and Engineering, Chungju National University, Chungju, Chungbuk 380-702, Korea

² Energy Materials Lab., Green Ceramic Division, Korea Institute of Ceramic Engineering and Technology, Seoul 153-801, Korea

³ The 4th R&D Institute-4, Agency for Defense Development, Daejeon 305-600, Korea

* Corresponding author (ihkim@cjnu.ac.kr)

Keywords: *thermoelectric, bismuth telluride, dispersion, nanocomposite*

1 Introduction

Thermoelectric materials are potential sources of electrical power from heat energy. Superior thermoelectric materials require a high Seebeck coefficient (α), a high electrical conductivity (σ) and a low thermal conductivity (κ) at application temperature (T in Kelvin) for a high figure of merit (Z):

$$ZT = \frac{\alpha^2 \sigma T}{\kappa} \quad (1)$$

which is related to thermoelectric energy conversion efficiency. The quantity $\alpha^2 \sigma$ is called the power factor and is the key to achieve high performance. The thermal conductivity has contributions from lattice vibrations and charge carrier transportations, and a low thermal conductivity is needed to maintain a temperature difference between hot and cold junctions of thermoelectric materials.

There are two approaches to increase ZT [1]. One is to maximize the power factor by developing new classes of thermoelectric materials, optimizing existing materials through doping, and exploring nanoscale materials. The other is to minimize the thermal conductivity by developing materials with intrinsically low thermal conductivity, solid-solution alloying, and realizing nanostructure engineering. Phonon glass and electron crystal (PGEC) concept is considered to reduce the thermal conductivity with maintaining the high power factor by introducing nanostructure or nanocomposite [2]. If the nanoparticles are well-dispersed and sufficiently small to intensify phonon scattering without

increasing charge carrier scattering, the figure of merit can be enhanced [3,4].

In general, however, the thermal conductivity reduction by phonon scattering accompanies the electrical conductivity reduction by charge carrier scattering due to inhomogeneous distribution and agglomeration of nanoparticles [5,6]. Conventional mixing process such as ball milling cannot provide appropriate nanostructure to realize the PGEC effect effectively in nanocomposites. In this study, a novel and simple approach was employed to disperse nanoparticles (Cu) uniformly in the matrix ($\text{Bi}_2\text{Te}_{2.7}\text{Se}_{0.3}$), and the thermoelectric properties were evaluated for the Cu-dispersed $\text{Bi}_2\text{Te}_{2.7}\text{Se}_{0.3}$ nanocomposites.

2 Experimental Procedure

Polycrystalline $\text{Bi}_2\text{Te}_{2.7}\text{Se}_{0.3}$ ingot was prepared by melting at 1073 K for 4 h with high purity (99.999 %) Bi, Te and Se granules in an evacuated quartz ampoule. The ingot was crushed into powder and sieved to obtain $< 75 \mu\text{m}$ diameter particles. $\text{Bi}_2\text{Te}_{2.7}\text{Se}_{0.3}$ powder was dry-mixed with $\text{Cu}(\text{OAc})_2$ powder. The mixture of $\text{Bi}_2\text{Te}_{2.7}\text{Se}_{0.3}$ and $\text{Cu}(\text{OAc})_2$ was then transferred to an alumina crucible and heated at 573 K for 3 h in a vacuum to decompose $\text{Cu}(\text{OAc})_2$. It was converted into Cu nanoparticles, which were chemically bonded to $\text{Bi}_2\text{Te}_{2.7}\text{Se}_{0.3}$ powder. Cu-dispersed $\text{Bi}_2\text{Te}_{2.7}\text{Se}_{0.3}$ nanocomposites were hot-pressed in a cylindrical graphite die with an internal diameter of 10 mm at 673 K under a pressure of 70 MPa for 1 h in a vacuum.

Scanning electron microscopy (SEM: FEI Quanta400) equipped with an energy dispersive

spectrometer (EDS) was used to observe the microstructure. Phase analysis was performed by X-ray diffraction (XRD: Bruker D8 Advance) using Cu K α radiation (40 kV, 40 mA). Diffraction patterns were measured in the θ -2 θ mode (10 to 90 degrees) with a step size of 0.02 degree, a scan speed of 0.2 degree/minute and a wavelength of 0.15405 nm. Hall effect measurements were carried out in a constant magnetic field (1 T) and electric current (50 mA) with Keithley 7065 system at room temperature to examine the carrier concentration and mobility. The Seebeck coefficient and electrical conductivity were measured using temperature differential and 4-probe methods, respectively, with Ulvac-Riko ZEM3 equipment in a helium atmosphere. The thermal conductivity was estimated from the thermal diffusivity, specific heat and density measurements using a laser flash Ulvac-Riko TC9000H system in a vacuum. The thermoelectric figure of merit was evaluated.

3 Results and Discussion

Fig. 1 shows the XRD patterns of Cu-dispersed Bi₂Te_{2.7}Se_{0.3} nanocomposites consolidated by hot pressing. Diffraction peaks were well-matched with the ICDD standard data. All samples were polycrystalline and Bi₂Te_{2.7}Se_{0.3} phase was successfully synthesized in this process. Diffraction peaks for Cu particles were not identified because the amount of Cu was too small to identify.

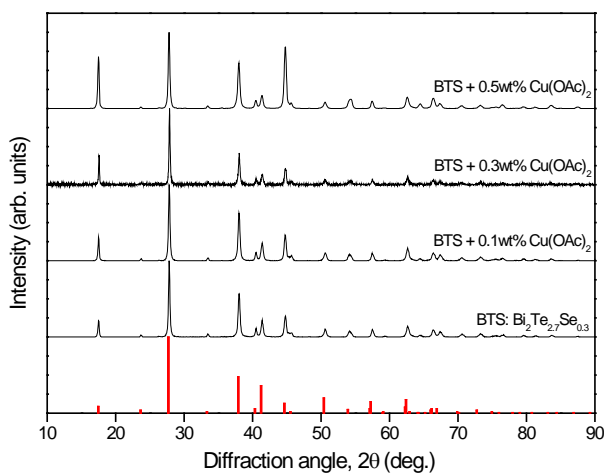


Fig.1. X-ray diffraction patterns of Cu-dispersed Bi₂Te_{2.7}Se_{0.3} nanocomposites.

Fig. 2 presents a SEM image of Cu-dispersed Bi₂Te_{2.7}Se_{0.3} nanocomposite prepared by Cu(OAc)₂ decomposition. Mean particle size of Cu is approximately 50 nm, and Cu nanoparticles are well-dispersed and bonded to the Bi₂Te_{2.7}Se_{0.3} powder surface.

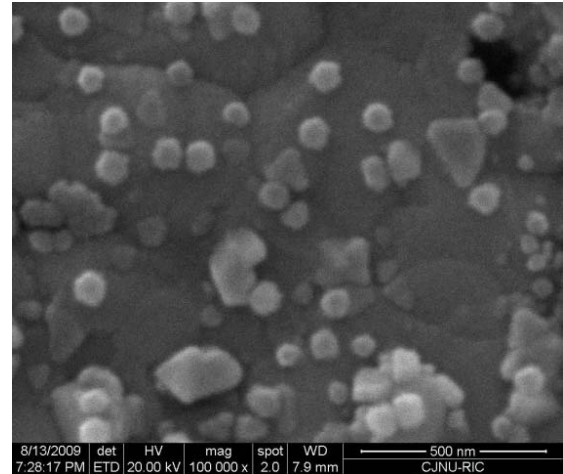


Fig.2. Cu-dispersed Bi₂Te_{2.7}Se_{0.3} nanocomposite prepared by Cu(OAc)₂ decomposition.

Fig. 3 shows the electrical conductivity of Cu-dispersed Bi₂Te_{2.7}Se_{0.3}. The electrical conductivity did not change significantly by Cu nanoparticle dispersion. It showed high-10⁴ S/m all temperatures examined, and which means that all specimens are in a degenerate state.

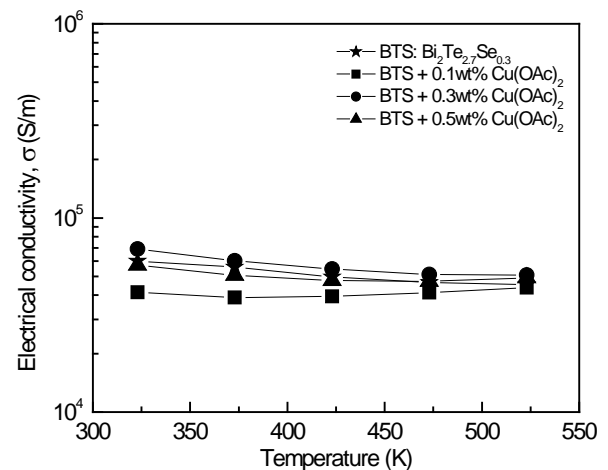


Fig.3. Electrical conductivity of Cu-dispersed Bi₂Te_{2.7}Se_{0.3}.

In order to examine the electronic transport properties, the Hall coefficient (R_H), carrier concentration (n) and mobility (μ) were measured. Table 1 lists the electronic transport properties of Cu-dispersed $\text{Bi}_2\text{Te}_{2.7}\text{Se}_{0.3}$ at room temperature. The sign of the Hall coefficient was negative for all specimens and it means that the electrical charge was transported mainly by electrons. The carrier concentration and mobility did not change significantly with Cu dispersion, which indicates that Cu nanoparticles are too small to introduce the charge carrier scattering.

Table 1. Electronic transport properties of Cu-dispersed $\text{Bi}_2\text{Te}_{2.7}\text{Se}_{0.3}$ at room temperature.

specimen	R_H (cm^3/C)	n (cm^{-3})	μ (cm^2/Vs)	m^* (m_0)
BTS	-0.134	4.7×10^{19}	80.4	0.91
BTS + 0.1 wt% $\text{Cu}(\text{OAc})_2$	-0.177	3.5×10^{19}	73.1	1.10
BTS + 0.3 wt% $\text{Cu}(\text{OAc})_2$	-0.145	4.3×10^{19}	99.9	1.12
BTS + 0.5 wt% $\text{Cu}(\text{OAc})_2$	-0.177	3.5×10^{19}	101.0	1.10

Fig. 4 presents the Seebeck coefficient of Cu-dispersed $\text{Bi}_2\text{Te}_{2.7}\text{Se}_{0.3}$. All specimens had a negative Seebeck coefficient, which confirmed that the electrical charge was transported mainly by electrons as shown in Table 1. The absolute Seebeck coefficient of $\text{Bi}_2\text{Te}_{2.7}\text{Se}_{0.3}$ was almost constant with temperature ranging 323–523 K. However, it was remarkably increased by Cu dispersion and slightly reduced with increasing temperature. The Seebeck coefficient is affected by the carrier concentration (n) and the effective mass (m^*) [7]:

$$\alpha = \frac{8\pi^2 k_B^2}{3eh^2} \left(\frac{\pi}{3n} \right)^{2/3} m^* T \quad (2)$$

where k_B , h and e are the Boltzmann constant, Planck constant and electrical charge, respectively.

In this study, because the carrier concentration did not change significantly, the increase in the Seebeck coefficient was due to the increase in the effective mass of a carrier, which is one of the critical factors determining the Seebeck coefficient. It is speculated that the charge-carrier energy filtering effect of the nanoparticles causes the increase in the effective

mass [8]. Therefore, as shown in Fig. 5, the power factor values for Cu-dispersed $\text{Bi}_2\text{Te}_{2.7}\text{Se}_{0.3}$ were maintained higher in the whole temperature range, and the maximum power factor at 323 K reached around two times higher than that of $\text{Bi}_2\text{Te}_{2.7}\text{Se}_{0.3}$.

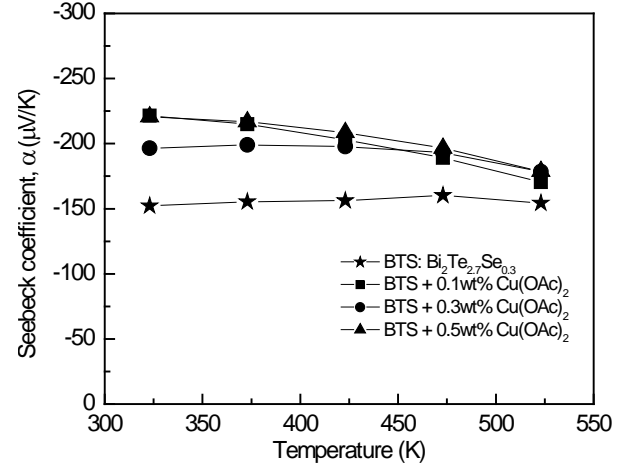


Fig.4. Seebeck coefficient of Cu-dispersed $\text{Bi}_2\text{Te}_{2.7}\text{Se}_{0.3}$.

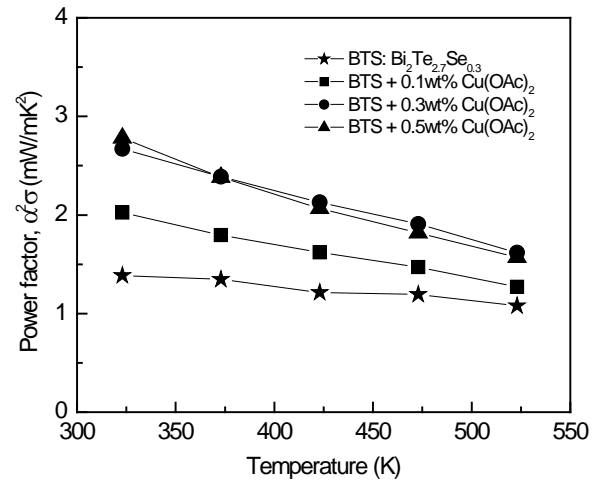


Fig.5. Power factor of Cu-dispersed $\text{Bi}_2\text{Te}_{2.7}\text{Se}_{0.3}$.

Fig. 6 shows the thermal conductivity of Cu-dispersed $\text{Bi}_2\text{Te}_{2.7}\text{Se}_{0.3}$. It was slightly increased with increasing temperature because of the electronic contribution, and Cu dispersion could not reduce it. The thermal conductivity (κ) is the sum of the lattice thermal conductivity (κ_L) by phonons and the electronic thermal conductivity (κ_E) by carriers, and it is given by Eq. 3:

$$\kappa = \kappa_L + \kappa_E = \kappa_L + L\sigma T \quad (3)$$

Both components can be separated by the Wiedemann-Franz law ($\kappa_E = L\sigma T$), where the Lorenz number is assumed to be a constant ($L = 2.0 \times 10^{-8} \text{ V}^2\text{K}^{-2}$) for evaluation [9,10].

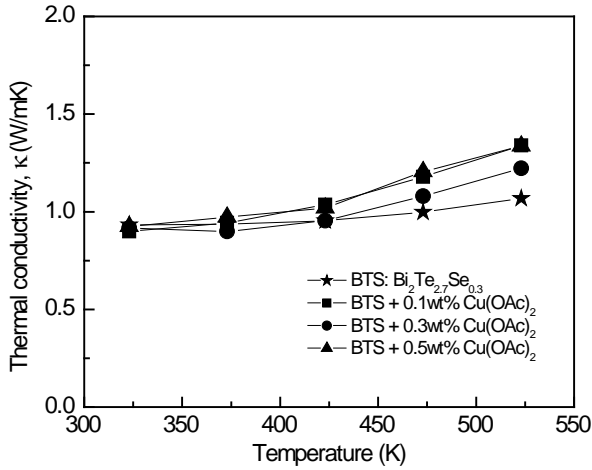


Fig.6. Thermal conductivity of Cu-dispersed $\text{Bi}_2\text{Te}_{2.7}\text{Se}_{0.3}$.

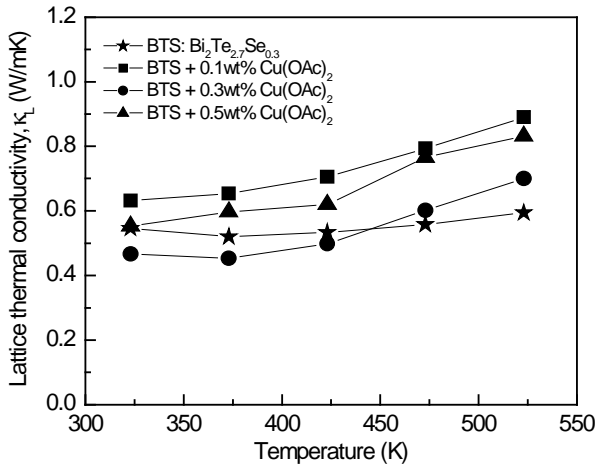


Fig.7. Lattice thermal conductivity of Cu-dispersed $\text{Bi}_2\text{Te}_{2.7}\text{Se}_{0.3}$.

The lattice thermal conductivity reduction was expected by the enhancement of phonon scattering at large density of incoherent interfaces which is created between $\text{Bi}_2\text{Te}_{2.7}\text{Se}_{0.3}$ matrix and Cu nanoparticles. However, as shown in Fig. 7, the well-controlled incoherent interfaces could not behave as effective phonon scattering centers, while several reports suggested that coherent interfaces are

essential to realize the PGEC effect effectively [3,4]. Although the lattice thermal conductivity decreased with increasing the amount of Cu dispersion, it was higher than that of $\text{Bi}_2\text{Te}_{2.7}\text{Se}_{0.3}$ excepting the specimen with 0.3 wt% $\text{Cu}(\text{OAc})_2$ below 423 K.

In order to obtain a maximum phonon scattering in the metal nanoparticle dispersion systems, the following issues remained for further investigations: the size control of metal nanoparticles, interface reaction control to form coherent interfaces with $\text{Bi}_2\text{Te}_{2.7}\text{Se}_{0.3}$ matrix and metal nanoparticles, and composition control of nanoinclusions.

Fig. 8 presents the temperature dependence of ZT for Cu-dispersed $\text{Bi}_2\text{Te}_{2.7}\text{Se}_{0.3}$ nanocomposites. ZT was enhanced dramatically by the Cu nanoparticle dispersion, which was mainly attributed to the increase in the power factor. The maximum ZT was obtained for 0.3 wt% $\text{Cu}(\text{OAc})_2$ added $\text{Bi}_2\text{Te}_{2.7}\text{Se}_{0.3}$ nanocomposite. Compared to $\text{Bi}_2\text{Te}_{2.7}\text{Se}_{0.3}$, ZT was remarkably improved by 50-200 % at the wide temperature range of 323-523 K.

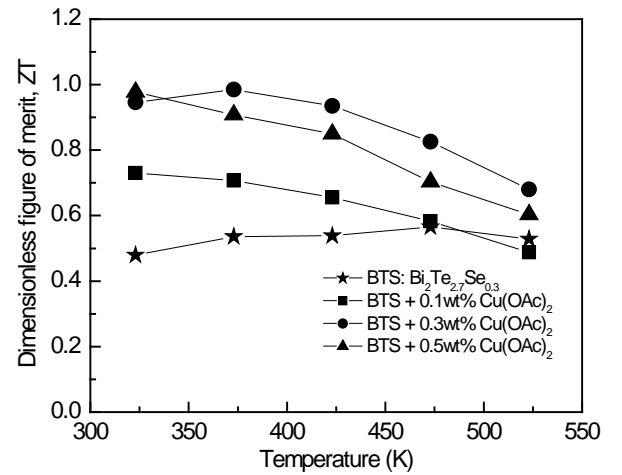


Fig.8. Thermoelectric figure-of-merit of Cu-dispersed $\text{Bi}_2\text{Te}_{2.7}\text{Se}_{0.3}$.

4 Conclusions

Cu-dispersed $\text{Bi}_2\text{Te}_{2.7}\text{Se}_{0.3}$ nanocomposites were prepared successfully by $\text{Cu}(\text{OAc})_2$ decomposition and hot pressing. Cu nanoparticles were well-dispersed in the $\text{Bi}_2\text{Te}_{2.7}\text{Se}_{0.3}$ matrix, and thereby the power factor was greatly increased due to increase in the effective mass of a carrier. However, Cu dispersion did not affect the carrier concentration and could not reduce the lattice thermal conductivity

because Cu nanoparticles did not act as phonon scattering centers effectively. Thermoelectric figure of merit was enhanced remarkably over wide temperature range of 323-523 K due to high power factor. Compared to other complex nanostructuring approaches, this metal nanoparticle dispersion method is simple and cost-effective for improving thermoelectric performance.

Acknowledgments

This work was supported by the Agency for Defense Development (UE105118GD), Republic of Korea.

References

- [1] J. R. Sootsman, D. Y. Chung, M. G. Kanatzidis, *Angew. Chem.*, Vol. 48, p. 8616, 2009.
- [2] G. A. Slack, “*CRC Handbook of Thermoelectrics*”, ed. by D. M. Rowe, CRC Press, Boca Raton, p. 407, 1995.
- [3] N. Mingo, D. Hauser, N. P. Kobayashi, M. Plissonnier, A. Shakouri, *Nano Lett.*, Vol. 9, p. 711, 2009.
- [4] G. Joshi, H. Lee, Y. Lan, X. Wang, G. Zhu, D. Wang, R. W. Gould, D. C. Cuff, M. Y. Tang, M. S. Dresselhaus, G. Chen, Z. Ren, *Nano Lett.*, Vol. 8, p. 4670, 2008.
- [5] Z. He, C. Stiewe, D. Platzek, G. Karpinski, E. Müller, *J. Appl. Phys.*, Vol. 101, p. 43707, 2007
- [6] J. F. Li, J. Liu, *Phys. Stat. Sol. A*, Vol. 203, p. 3768, 2006.
- [7] G. J. Snyder, E. S. Toberer, *Nature Mater.*, Vol. 7, p. 105, 2008.
- [8] S. V. Faleev, F. Léonard, *Phys. Rev. B*, Vol. 77, p. 21304, 2008.
- [9] R. Venkatasubramanian, E. Siivola, T. Colpitts, B. O’Quinn, *Nature*, Vol. 11, p. 597, 2001.
- [10] J. E. Parrott, A. D. Stukes, *Thermal Conductivity of Solids*, Pion, p. 80, 1975.